Resonance fluorescence near a photonic band edge: Dressed-state Monte Carlo wave-function approach

Tran Quang and Sajeev John
Department of Physics, University of Toronto, 60 St. George Street, Toronto, Ontario, Canada M5S 1A7
(Received 2 June 1997)

We introduce a dressed-state Monte Carlo wave-function technique to describe resonance fluorescence in a broad class of non-Markovian reservoirs with strong atom-reservoir interaction. The method recaptures photon localization effects which are beyond the Born and Markovian approximations, and describes the influence of the driving field on the atom-reservoir interaction. Using this approach, we predict a number of fundamentally new features in resonance fluorescence near the edge of a photonic band gap. In particular, the atomic population exhibits inversion for moderate applied field intensity. For a low external field intensity, the atomic system retains a long-time memory of its initial state. [S1050-2947(97)09711-4]

PACS number(s): 42.50.Lc, 42.50.Hz, 32.80.−t

Localization of light [1] in photonic band-gap (PBG) materials [2,3] gives rise to fundamentally new effects in atom-radiation field interactions. In recent years, several dielectric structures have been predicted [2–5] and observed [6–10] to exhibit a photonic band gap, a range of frequencies for which no propagating electromagnetic modes are allowed. This existence of PBG materials gives rise to a number of interesting phenomena including inhibition of spontaneous emission [2,11,12], strong localization of light, and formation of atom-photon bound state [3,13,14]. Other confined photonic systems [15–18] such as microcavities, optical fibers, and optical wires also exhibit novel features arising from our ability to tailor the photon density of states (DOS) in a prescribed manner. The distinguishing common feature of the confined photonic systems is that the photonic mode density exhibits a rapid variation with frequency at certain edge or cutoff frequencies. For example, in the optical fibers, the mode density vanishes abruptly below a waveguide cutoff frequency ω_0. For $\omega \geqslant \omega_0$, the mode density of the fiber diverges as $(\omega-\omega_0)^{-1/2}$ [18]. In photonic band-gap materials, the DOS exhibits band-edge and other van Hove singularities. At the band-edge frequency $\omega_{\rm edge}$, this can take the form of a singularity of the form $|\omega-\omega_{\rm edge}|^{-1/2}$ (one-dimensional or isotropic PBG), step discontinuity (two-dimensional PBG), or a singularity of the form $|\omega-\omega_{\rm edge}|^{1/2}$ in a anisotropic three-dimensional PBG [13].

Photon localization near the singularity of the mode density of a PBG leads to a novel regime of strong interaction between atoms and the radiation reservoir. In this situation, the Born and Markov approximations normally used in deriving master equation for atomic systems [19] are invalid. Recent attempts using only the Born approximation [20,21] failed to capture the effects of light localization and vacuum Rabi splitting of the atomic level near a photonic band edge. Moreover, the rapid variation of the photon mode density may lead to a dramatic influence of an applied field on the atom-reservoir interaction as a result of the different DOS's at the different dressed-state transition frequencies. The effect of the applied field on the atom-reservoir interaction has been discussed previously [22–25] in the framework of Born and Markovian approximations. This, however, is inadequate for the case when the dressed-state transition frequencies remain close to cutoff or edge frequencies.

In this paper we introduce a dressed-state Monte Carlo wave-function (MCWF) technique [26–28] for a wide class of non-Markovian atom radiation reservoir interactions. This method overcomes the shortcomings of the Born and Markovian approximations, and captures the influence of the driving field on the atom-reservoir interaction. Using this technique, we find new rich features of resonance fluorescence near the band edge of a PBG. In contrast to free-space resonance fluorescence, atomic population inversion occurs for a moderate intensity of the applied field. Furthermore, we show that, for a low intensity of the driving field, the atomic system keeps a long-time memory of its initial state. This may be relevant to an optical memory device at the atomic scale.

Consider a system of a two-level atoms driven by a classical external laser field and coupled to the radiation field reservoir. The atoms have an excited state $|2\rangle$, ground state $|1\rangle$, and resonant transition frequency ω_{21}. The Hamiltonian of the system in the interaction picture takes the form $H=H_0+H_1$, where

$$H_0=\tfrac{1}{2}\hbar\Delta(\sigma_{22}-\sigma_{11})+\hbar\varepsilon(\sigma_{12}+\sigma_{21})+\sum_\lambda \hbar\delta_\lambda a_\lambda^\dagger a_\lambda, \tag{1}$$

$$H_1=i\hbar\sum_\lambda g_\lambda(a_\lambda^\dagger\sigma_{12}-\sigma_{21}a_\lambda). \tag{2}$$

Here $\sigma_{ij}=|i\rangle\langle j|$ $(i,j=1,2)$ are the atomic operators; a_λ and $a_\lambda^\dagger$ are the radiation field annihilation and creation operators; $\Delta=\omega_{21}-\omega_L$; $\delta_\lambda=\omega_\lambda-\omega_L$; ω_L and ω_λ are the applied field frequency and the frequency of a mode λ, respectively; ε is the resonant Rabi frequency of the applied field; and g_λ is the atom-radiation field coupling constant.

To include the role of the applied field on atom-reservoir interaction, we use the basis of dressed states $|\widetilde{1}\rangle=c|1\rangle-s|2\rangle$, $|\widetilde{2}\rangle=s|1\rangle-c|2\rangle$. Here $c\equiv\cos\phi$, $s\equiv\sin\phi$, and $\sin^2\phi=\frac{1}{2}[1-\mathrm{sgn}(\Delta)/(4\varepsilon^2/\Delta^2+1)^{1/2}]$. This leads to the dressed-state Hamiltonian [25]

$$H_0=\hbar\Omega(R_{22}-R_{11})+\sum_\lambda \hbar\delta_\lambda a_\lambda^\dagger a_\lambda, \tag{3}$$

where $\Omega=(\varepsilon^2+\Delta^2/4)^{1/2}$ and $R_{ij}=|\widetilde{i}\rangle\langle\widetilde{j}|$ $(i,j=1,2)$ are the dressed atomic operators. In the dressed-state basis $|\widetilde{i}\rangle$, σ_{21} in the interaction Hamiltonian H_1 must be replaced by $\sigma_{21}=cs(R_{22}-R_{11})+c^2R_{21}-s^2R_{12}$, and the atomic population on the bare state $|2\rangle$ can be written as $\langle\sigma_{22}\rangle=s^2\langle R_{11}\rangle+c^2\langle R_{22}\rangle-2cs\ \mathrm{Re}(\langle R_{12}\rangle)$. We define the time-dependent interaction picture Hamiltonian $\widetilde{H}_1(t)=U^\dagger(t)H_1U(t)$ where $U(t)=\exp(-iH_0t/\hbar)$. In this interaction picture, the interaction Hamiltonian $\widetilde{H}_1$ takes the form

$$\widetilde{H}_1=i\hbar\sum_\lambda g_\lambda[a_\lambda^\dagger(csR_3e^{i\delta_\lambda t}+c^2R_{12}e^{i(\delta_\lambda-2\Omega)t} -s^2R_{21}e^{i(\delta_\lambda+2\Omega)t})-\mathrm{H.c.}], \tag{4}$$

To determine the dynamics of this problem in an amplitude picture, we consider the projection of the atomic dressed-state wave function onto the one-photon sector of the full Hilbert space,

$$|\Psi(t)\rangle_{AF}=b_1(t)|\widetilde{1}\rangle\otimes|\mathrm{vac}\rangle+\sum_\lambda b_{1\lambda}(t)|\widetilde{1}\rangle\otimes a_\lambda^\dagger|\mathrm{vac}\rangle +b_2(t)|\widetilde{2}\rangle\otimes|\mathrm{vac}\rangle+\sum_\lambda b_{2\lambda}(t)|\widetilde{2}\rangle\otimes a_\lambda^\dagger|\mathrm{vac}\rangle. \tag{5}$$

The process of resonance fluorescence, however, spans the multiphoton sector of the atom-radiation field Hilbert space, since energy absorbed by the atom from the external laser field can be re-emitted by the process of spontaneous and stimulated emission. That is, the state vector $|\Psi\rangle_{AF}$ fails to capture the possibility of random repopulation of the atomic ground state with many photons scattered into the radiation field reservoir. In what follows, the multiphoton contribution in repopulation of the ground state will be added in terms of a Monte Carlo simulation. The time-dependent Schrödinger equation, projected on the one-photon sector of the Hilbert space, takes the form

$$\frac{d}{dt}b_1(t)=cs\sum_\lambda g_\lambda b_{1\lambda}e^{-i\Delta_\lambda t}+s^2\sum_\lambda g_\lambda b_{2\lambda}e^{-i(\Delta_\lambda+2\Omega)t}, \tag{6}$$

$$\frac{d}{dt}b_2(t)=-c^2\sum_\lambda g_\lambda b_{1\lambda}e^{-i(\Delta_\lambda-2\Omega)t}-cs\sum_\lambda g_\lambda b_{2\lambda}e^{-i\Delta_\lambda t}, \tag{7}$$

$$\frac{d}{dt}b_{1\lambda}(t)=-csg_\lambda b_1e^{i\Delta_\lambda t}+c^2g_\lambda b_2e^{i(\Delta_\lambda-2\Omega)t}, \tag{8}$$

$$\frac{d}{dt}b_{2\lambda}(t)=-s^2g_\lambda b_1e^{i(\Delta_\lambda+2\Omega)t}+csg_\lambda b_2e^{i\Delta_\lambda t}. \tag{9}$$

Substituting solutions of Eqs. (8) and (9) into Eqs. (6) and (7), we obtain,

$$\frac{d}{dt}b_1(t)=-c^2s^2\int_0^\infty G_0(t-t')b_1(t')dt'+cs^3e^{-2i\Omega t}\times\int_0^\infty G_0(t-t')b_2(t')dt'-s^4\int_0^\infty G_-(t-t')\times b_1(t')dt'+c^3se^{-2i\Omega t}\times\int_0^\infty G_+(t-t')b_2(t')dt', \tag{10}$$

$$\frac{d}{dt}b_2(t)=c^3se^{2i\Omega t}\int_0^\infty G_0(t-t')b_1(t')dt'-c^2s^2\times\int_0^\infty G_0(t-t')b_2(t')dt'+cs^3e^{2i\Omega t}\times\int_0^\infty G_-(t-t')b_1(t')dt'-c^4\int_0^\infty G_+(t-t')b_2(t')dt', \tag{11}$$

where $G_0(t-t')=\Sigma_\lambda g_\lambda^2e^{-i(\omega_\lambda-\omega_L)(t-t')}$ and $G_\pm(t-t')=\Sigma_\lambda g_\lambda^2e^{-i[\omega_\lambda-(\omega_L\pm2\Omega)](t-t')}$ are the delay Green's functions at the Mollow frequencies ω_L and $\omega_L\pm2\Omega$, respectively. In a system, such as a PBG material, with fast variation of the density of states in the frequency range $\omega_L-2\Omega$ to $\omega_L+2\Omega$, these Green's functions may be very different. This difference embodies the influence of the external applied field on the atom-reservoir interaction. For a strong external field, the dressed-state transition frequencies ω_L and $\omega_L\pm2\Omega$ may be pushed far away from the band-edge singularity. In this case, these Green's functions are proportional to the DOS at ω_L and $\omega_L\pm2\Omega$, and it is sufficient to solve the quantum dynamics in the Born and Markov approximations [22–25]. For weak and moderate external fields, the Mollow's spectral components remain close to the DOS singularity and it is essential to solve Eqs. (10) and (11) without recourse to the Born and Markovian approximations. Even for strong external field, the non-Markovian effects may cause new interesting features when one of the Mollow's spectral components is close to the DOS singularity.

In general, the Green's functions are determined by the structure of the density of states. For a broadband, smoothly varying density of state (as in free space), the dependence of the Green's functions on the applied field can be ignored: $G_0(t-t')=G_\pm(t-t')\sim(\gamma/2)\,\delta(t-t')$, where γ is the spontaneous emission rate of the atom. Equations (10) and (11) can be simplified to

$$\frac{d}{dt}b_1(t)=-(\gamma/2)s^2b_1(t)+(\gamma/2)cse^{-2i\Omega t}b_2(t), \tag{12}$$

$$\frac{d}{dt}b_2(t)=-(\gamma/2)c^2b_2(t)+(\gamma/2)cse^{2i\Omega t}b_1(t). \tag{13}$$

Equations (12) and (13) are equivalent to the quantum dynamics of the effective atomic (non-Hermitian) Hamiltonian [26–28]

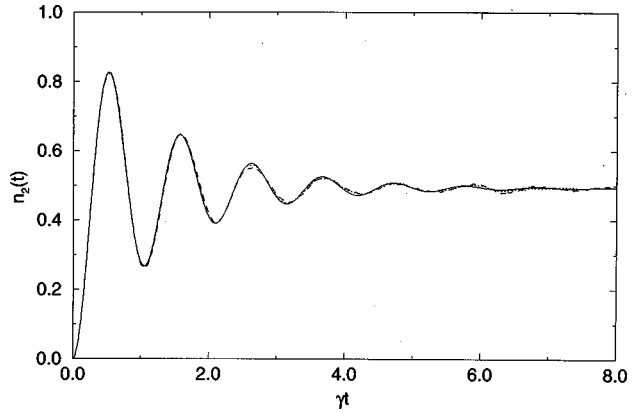

FIG. 1. Atomic population on the bare upper state, $n_2(t) = \langle \sigma_{22}(t) \rangle$, as functions of the scaled time γt for the ordinary vacuum case. Here $\Omega/\gamma = 3$, γ is the vacuum rate of spontaneous emission, Ω is Rabi frequency, and the detuning of the laser frequency from atomic resonance $\Delta = 0$. The number of realizations in the Monte Carlo simulation is $N = 5000$ (dashed curve) and $N = 10^4$ (dotted curve). The solid curve is an exact solution of the optical Bloch equation for the same choice of parameters.

$$H_{\text{eff}} = \tfrac{1}{2}\hbar\left(\Delta - i\,\frac{\gamma}{2}\right)\sigma_{22} - \tfrac{1}{2}\hbar\Delta\sigma_{11} + \hbar\varepsilon(\sigma_{12} + \sigma_{21}). \tag{14}$$

In other words, Eqs. (12) and (13) can be derived from Eq. (14) using the dressed-state atomic state vector in the form

$$|\Psi(t)\rangle = b_2(t)|\widetilde{2}\rangle + b_1(t)|\widetilde{1}\rangle. \tag{15}$$

We emphasize that Eqs. (10)–(13) describe only the single-photon sector of the Hilbert space, and do not describe the actual repopulation of the ground state after many photons have been scattered into the reservoir. Consequently, the norm of the dressed-state wave function $P(t) = |b_1(t)|^2 + |b_2(t)|^2$ changes with time. It has been shown that this inadequacy may be overcome by recourse to a Monte Carlo wave-function technique [26–28]. In this method, the atomic system can be described by the normalized wave function ''no-jump state vector''

$$|\widetilde{\Psi}(t)\rangle = \frac{b_2(t)}{\sqrt{P(t)}}\,|\widetilde{2}\rangle + \frac{b_1(t)}{\sqrt{P(t)}}\,|\widetilde{1}\rangle, \tag{16}$$

in which the evolution of the system from its initial state [$b_1(0) = c$, $b_2(0) = s$ if atom is initially in its bare ground state and $b_1(0) = -s$, $b_2(0) = c$ if atom is initially in its bare excited state] is determined in a piecewise manner by Eqs. (10) and (11). At random instants of time t_i, this evolution is interrupted by a quantum jump (spontaneous emission event) that reduces the atomic wave function to the ground state. The system then evolves further from its bare ground state [with $b_1(t_i) = c$ and $b_2(t_i) = s$] according Eqs. (10) and (11) until the next random jump. For each piecewise time evolution of the system (realization), we calculate the outer product $|\widetilde{\Psi}(t)\rangle\langle\widetilde{\Psi}(t)|$. Repeating the above simulation N realizations, we obtain an approximate dressed-state atomic density matrix $\rho_A(t) = (1/N)\Sigma_1^N |\widetilde{\Psi}(t)\rangle\langle\widetilde{\Psi}(t)|$. In our numerical simulation, the jump was imposed when the norm $P(t)$ was

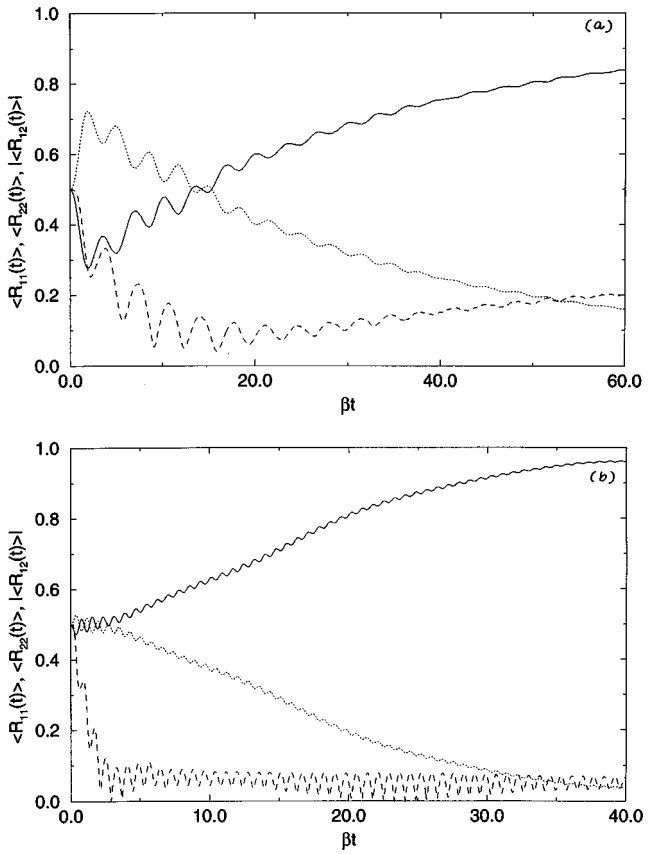

FIG. 2. (a) Atomic population on the lower and upper dressed states, $\langle R_{11}(t) \rangle$ (solid curve) and $\langle R_{22}(t) \rangle$ (dotted curve), and the amplitude of the dressed-state atomic polarization $|\langle R_{12}(t) \rangle|$ (dashed curve) as a function of a scaled time βt. Here both the detuning of the laser frequency from the atomic resonance, Δ, and the detuning of laser frequency from the band-edge frequency, $\delta_0 \equiv \omega_L - \omega_c$, are equal to zero. The number of Monte Carlo realizations $N = 5000$ and the external Rabi frequency $\Omega/\beta = 0.8$. The atom is initially in its bare ground state. (b) Same as (a), except for an external strong field $\Omega/\beta = 4$.

equal to a random number η chosen uniformly on the interval between zero and unity [27]. That is to say, after any given jump a new random number η is chosen to prescribe the time of the subsequent jump.

As an illustration for the dressed-state MCWF technique for Markovian systems, in Fig. 1 we plot the probability of the atom on the bare excited state $n_2(t) = \langle \sigma_{22}(t) \rangle$ in an ordinary vacuum (dashed and dotted curves), and compare this with the exact solution of the optical Bloch equation (solid curve) [29] for $\Omega = 3\gamma$ and $\Delta = 0$. Clearly, for a large number of realizations ($N = 10^4$ for the dotted curve), the simulation result is indistinguishable from the exact solution.

The simulation of the dressed-state MCWF for a reservoir with a singular DOS and non-Markovian noise can be carried out analogously. The only difference in this case is the form of the Green's function $G_0(t - t')$ and $G_{\pm}(t - t')$. As an illustration of the dressed-state MCWF technique for non-Markovian system, we choose an isotropic PBG described by the effective-mass dispersion relation near the band-edge frequency ω_c: $\omega_k = \omega_\lambda \cong \omega_c + A(k - k_0)^2$, with $A \cong \omega_c/k_0^2$ [13,14]. Using this dispersion relation, the delay Green's functions take the forms

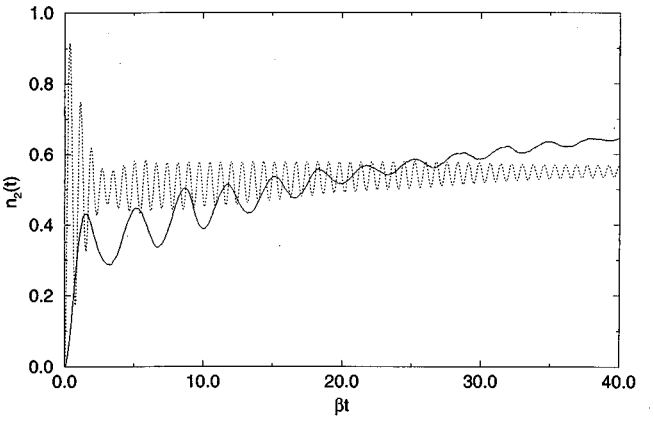

FIG. 3. Atomic population on the bare upper state, $n_2(t)$, as a function of a scaled time βt for $\Delta=\delta_0=0$ and $N=5000$. Here $\Omega/\beta=0.8$ (solid curve) and $\Omega/\beta=4$ (dotted curve). In both cases, the atom is initially in its bare ground state.

$$G_0(t-t')=\beta^{3/2}e^{i\delta_0(t-t')-i\pi/4}/\sqrt{\pi(t-t')}, \tag{17}$$

$$G_{\pm}(t-t')=\beta^{3/2}e^{i\delta_{\pm}(t-t')-i\pi/4}/\sqrt{\pi(t-t')}, \tag{18}$$

where $\delta_0=\omega_L-\omega_c$, $\delta_{\pm}=\omega_L\pm 2\Omega-\omega_c$ and $\beta^{3/2}=\omega_{21}^{7/2}d^2/(6\pi\varepsilon_0\hbar c^3)$, where ε_0 is the Coulomb constant and d is the atomic dipole moment [11]. Following the Monte Carlo numerical simulation described above and the Green's function Eqs. (17) and (18), we obtain an approximate atomic density matrix $\rho_A(t)$. This density matrix is then used to evaluate expectation values of dressed-state and bare atomic operators.

In Fig. 2, we plot atomic populations $\langle R_{11}(t)\rangle$ and $\langle R_{22}(t)\rangle$ on the dressed states $|\tilde{1}\rangle$ and $|\tilde{2}\rangle$, respectively, as a function of a scaled time βt for the case when the atomic resonance frequency ω_{21} and the laser frequency are at the edge frequency ω_c ($\Delta=\delta_0=0$) for moderate [Fig. 2(a)] and strong [Fig. 2(b)] external fields. For the exact resonance case ($\Delta=0$) in ordinary vacuum [29], $\langle R_{11}\rangle=\langle R_{22}\rangle=\frac{1}{2}$ in the long-time limit. In a PBG, the dressed state $|\tilde{1}\rangle$ (the left Mollow's sideband with frequency $\omega_c-2\Omega$ [29,30]) is inside the gap and exhibits negligible decay, whereas the dressed state $|\tilde{2}\rangle$ (the right Mollow's sideband at the frequency $\omega_c+2\Omega$) is outside the gap and exhibits resonance fluorescence. Consequently, in the long-time limit, the atomic population on the dressed state $|\tilde{1}\rangle$ is much larger than the atomic population in the dressed state $|\tilde{2}\rangle$, as shown in Figs. 2(a) and 2(b). This imbalance of the atomic population between dressed states modifies the spectrum of resonance fluorescence considerably. In particular, the left sideband is absent because of the negligible DOS inside the gap. The total intensity of the right sideband, which is proportional to $\langle R_{21}R_{12}\rangle=\langle R_{22}\rangle$, is also suppressed (relative to the corresponding Mollow sideband in free space) as a result of the decrease in $\langle R_{22}\rangle$ [solid curves in Figs. 2(a) and 2(b)]. At a very strong applied field, both sidebands are almost totally suppressed, in agreement with Ref. [22].

The atomic population on the upper bare state $|2\rangle$ also exhibits new features. In Fig. 3, we plot $n_2(t)=\langle\sigma_{22}\rangle$ as a function of βt for the same parameters as in Fig. 2. Clearly, the steady-state atomic population exhibits inversion ($\langle\sigma_{22}\rangle$

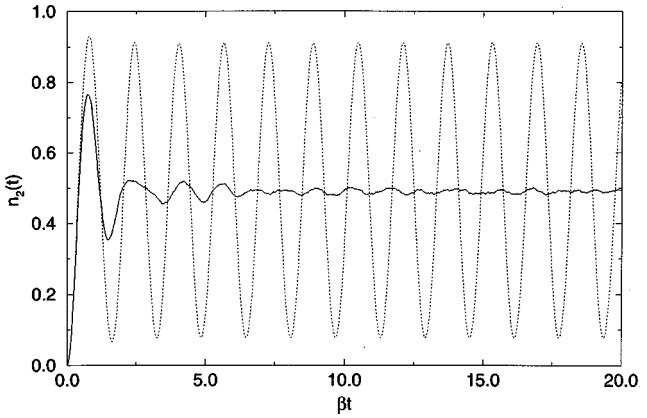

FIG. 4. Atomic population on the bare upper state, $n_2(t)$, as a function of a scaled time βt for $\Delta=0$, $N=5000$, and $\Omega/\beta=2$. Here the detuning of the laser frequency from the band edge is given by $\delta_0/\beta=5$ (solid curve) and $\delta_0/\beta=-5$ (dotted curve). The atom is initially in the bare ground state.

$>1/2$) for the moderate value of the resonant Rabi frequency $\Omega/\beta=0.8$ (solid curve). This atomic population inversion cannot be obtained in the framework of resonance fluorescence in ordinary vacuum. Unlike conventional lasers, which require the existence of additional atomic levels to achieve inversion, atomic population inversion may occur for a photonic band-gap laser using two-level atoms and moderate coherent pumping. At a strong resonant external field, the atomic system approaches a saturation state with small dressed-state atomic polarization [dashed curve in Fig. 2(b)] and small atomic population inversion (dotted curve in Fig. 3). The atomic population inversion has been discussed in Refs. [22,25] using the Markovian approximation, ignoring the effects of photon localization. In this paper, the band-edge localization effects are included. As a result, the atomic population exhibits inversion for much weaker applied field ($\Omega\leqslant\beta$) than that required in Refs. [22,25]. In Fig. 4 we plot the atomic population in the upper bare state $|2\rangle$ for the case when ω_{21} and ω_L are far outside the gap and far inside the gap. Clearly, outside the gap, the atomic system behaves as in an ordinary vacuum (solid curve). Inside the gap, $n_2(t)$

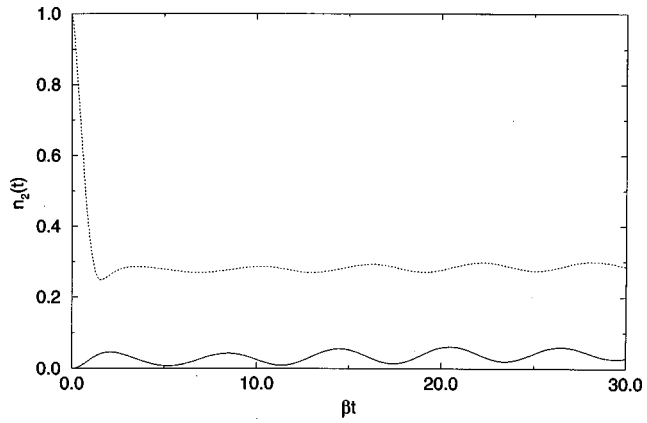

FIG. 5. Atomic population on the bare upper state, $n_2(t)$, as a function of a scaled time βt for $\Delta=\delta_0=0$, $N=5000$, and $\Omega/\beta=0.2$, for the case when the atom is initially in the bare excited state (dotted curve) and initially in the bare ground state (solid curve).

exhibits sinusoidal Rabi oscillations characteristic of a driven two-level system with very small spontaneous emission decay rate [29] (dotted curve).

In Fig. 5 we plot $n_2(t)$ for the non-Markovian case of a weak external field in which the atom is initially in the excited state (dotted curve) or initially in the ground state (solid curve). In the former case, the weak-field resonance fluorescence is strongly affected by localization of spontaneous emission [11]. This is manifest in the long-time behavior of the atomic system, which retains the memory of the initial state as shown in Fig. 5. This is distinct from free-space resonance fluorescence [29,30], where the long-time behavior of the atomic system is independent of its initial state. As such, the two-level atomic system in a PBG constitutes an optical memory device. For a multilevel atom interacting with more than one external laser field, the non-Markovian effects of photon localization facilitate a coherent control of spontaneous emission, and the steady-state atomic inversion depends sensitively on the relative phase between the laser fields [31]. On the other hand, for a strong external field $\Omega \gg \beta$, the external field itself dominates the dynamics, and the memory of the initial state on the long-time behavior of the atomic system is suppressed.

In conclusion, we have considered band-edge resonance fluorescence using a dressed-state MCWF technique. This approach overcomes the shortcomings of the Born and Markovian approximations, and the influence of the applied field on atom-reservoir interaction is accounted for. The dressed-state MCWF approach may be used for a broad class of non-Markovian reservoirs including PBG materials, optical fibers, and other confined photonic systems, where the appropriate non-Markovian master equation is difficult to solve. The new features of the band edge resonance fluorescence include the occurrence of the atomic population inversion and long-time memory of the initial state. The non-Markovian effects of photon localization described here suggest the possibility that collective switching of an N-atom system near a photonic band edge may occur at a much lower ($\Omega \leqslant \beta$) threshold than previously considered [25].

This work was supported in part by the Natural Sciences and Engineering Research Council of Canada and the Ontario Laser and Lightwave Research Centre, and by a grant from William F. McLean.

[1] S. John, Phys. Rev. Lett. **53**, 2169 (1984); Phys. Rev. B **31**, 304 (1985).
[2] E. Yablonovitch, Phys. Rev. Lett. **58**, 2059 (1987).
[3] S. John, Phys. Rev. Lett. **58**, 2486 (1987).
[4] K. M. Ho, T. J. Chan, and C. M. Soukoulis, Phys. Rev. Lett. **65**, 3152 (1990).
[5] J. D. Joannopoulos, P. R. Villeueuve, and S. Fan, Nature (London) **386**, 143 (1997).
[6] E. Yablonovitch, T. J. Gmitter, and K. M. Leung, Phys. Rev. Lett. **67**, 2295 (1991).
[7] U. Gruning, V. Lehmann, and C. M. Engelhardt, Appl. Phys. Lett. **66**, 3254 (1995); U. Gruning, V. Lehmann, S. Ottow, and K. Busch, *ibid.* **68**, 747 (1996).
[8] E. Ozbay, E. Michel, G. Tuttle, M. Sigala, R. Biswas, and K. M. Ho, Appl. Phys. Lett. **64**, 2059 (1994).
[9] R. Baughman and A. Zakhidov (private communication).
[10] For a review, see *Photonic Band Gap Materials*, Vol. 315 of *NATO Advanced Study Institute Series E: Applied Sciences*, edited by C. M. Soukoulis (Kluwer, Dordrecht, 1996).
[11] S. John and Tran Quang, Phys. Rev. A **50**, 1764 (1994).
[12] S. Bay, P. Lambropoulos, and K. Molmer, Opt. Commun. **132**, 257 (1996).
[13] S. John and J. Wang, Phys. Rev. Lett. **64**, 2418 (1990); Phys. Rev. B **43**, 12 772 (1991).
[14] S. John and Tran Quang, Phys. Rev. Lett. **74**, 3419 (1995).
[15] *Confined Electrons and Photons*, edited by E. Burstein and C. Weisbuch (Plenum, New York, 1995).
[16] S. Haroche and Kleppner, Phys. Today **42(1)**, 24 (1989).
[17] S. D. Brorson, H. Yokoyoma, and E. P. Ippen, IEEE J. Quantum Electron. **26**, 1492 (1990).
[18] D. Kleppner, Phys. Rev. Lett. **47**, 233 (1981).
[19] G. S. Agarwal, *Quantum Optics* (Springer-Verlag, Berlin, 1974).
[20] M. Lewenstein, T. M. Mossberg, and R. J. Glauber, Phys. Rev. Lett. **59**, 775 (1987).
[21] A. G. Kofman, G. Kurizki, and B. Sherman, J. Mod. Opt. **41**, 353 (1994).
[22] T. W. Mossberg and M. Lewenstein, J. Opt. Soc. Am. B **10**, 340 (1993).
[23] O. Kocharovskya, S. Y. Zhu, M. O. Scully, P. Mandel, and Y. V. Radeonychev, Phys. Rev. A **49**, 4928 (1994).
[24] C. H. Keitel, P. L. Knight, L. M. Narducci, and M. O. Scully, Opt. Commun. **118**, 143 (1995).
[25] S. John and Tran Quang, Phys. Rev. Lett. **78**, 1888 (1997).
[26] H. Carmichael, *An Open Systems Approach to Quantum Optics* (Springer, Berlin, 1993), and references therein.
[27] R. Dum, P. Zoller, and H. Ritsch, Phys. Rev. A **45**, 4879 (1992).
[28] J. Dalibard, Y. Castin, and K. Molmer, Phys. Rev. Lett. **68**, 580 (1992); P. Stenius and Imamoglu, Quantum Semiclassic. Opt. **8**, 283 (1996).
[29] C. Cohen-Tannoudji, J. Dupont-Roc, and G. Grynberg, *Atom-Photon Interactions* (Wiley-Interscience, New York, 1992), Chap. VI.
[30] B. M. Mollow, Phys. Rev. **188**, 1969 (1969).
[31] Tran Quang, M. Woldeyohannes, S. John, and G. S. Agarwal (unpublished).